The effect of size of Au-core Ag-shell nanoparticles on their enhancement of fluorescence

Fang Xie*, Ewa M. Goldys*
*Division of Information and Communication Sciences
Macquarie University, North Ryde, NSW 2109, Australia
Email: fangxie@ics.mq.edu.au
Telephone: (612) 98507747, Fax: (612) 98508115

Abstract—A simple method has been developed for homogeneous deposition of uniform Au-core Ag-shell nanoparticles on glass substrate. The method uses uniform gold colloid as seed and a silver enhancing kit to provide silver overlayer with improved fluorescence enhancement properties. Depending on size of these nanoparticles, the fluorescence of FITC-HSA monolayer deposited over the nanoparticles is either quenched, not affected or, enhanced in comparison to the control area - bare glass surface. Thus a pronounced size effect underpins the ability of these nanoparticles to enhance fluorescence. Nanostructures of appropriate size thus prepared can produce promising substrates for fluorescence enhancement. One of the outstanding advantages of this method is that such substrates are spatially homogeneous, which will pave the way for application of such substrates in biotechnology and life sciences.

Keywords- *Nanoparticle; MEF substrate; FITC-HSA conjugation*

I. INTRODUCTION

Fluorescence is uniquely suited to biological assays owing to its sensitivity, and thus it is rapidly becoming a leading method in medical diagnostics and biotechnology. To date many methods has been developed to increase the sensitivity of fluorescence detection [1-6]. Fluorescence amplification by metal nanostructures is a relatively new methodology which has been explored extensively over last five years [7-9]. Briefly, Metal Enhanced Fluorescence (MEF) is due to interactions of the excited fluorophores with surface plasmon resonances in metal nanostructured surfaces. Such structures produce desirable effects on fluorophores near the surface such as increased quantum yields, decreased lifetimes, increased photostability, and increased energy transfer. Various MEF substrates have been reported [8, 9], including silver island films, silver nanorods, and silver fractals.

We report here a new and simple approach to produce a MEF substrate leading to good uniformity. In this method, the Au colloid as seed is first covalently deposited on 3(aminopropyl)trimethoxysilane (APTMS)-coated glass substrate. Subsequently, the coated glass is immersed in a silver enhancing kit solution to form Au-core Ag-shell nanostructures. A monolayer of FITC-conjugated Human Serum Albumin (FITC-HSA) is then formed both on a silver nanoparticle covered glass surface as well as on a bare glass surface area as a control. Laser Scanning Microscopy at 488 nm excitation wavelength reveals the enhancement of fluorescence emission in the areas containing the nanoparticles as well as on bare glass surface without the nanoparticles. The SEM images proved that the substrates thus produced are spatially homogeneous, in contrast to the competing methods, which is of significance for real technological applications such as imaging and biosensing.

II. MATERIALS AND METHODS

Materials. The following materials were purchased from Sigma-Aldrich and used as received: $HAuCl_4 \bullet 3H_2O$, trisodium citrate dehydrate, (3-aminopropyl)trimethoxylsilane) trimethoxylsilane (APTMS), silver enhancing kit (silver enhancing solution A and silver enhancing solution B), and FITC conjugated human serum albumin (FITC-HSA). Concentrated HCl, HNO_3, H_2SO_4, and methanol were obtained from J. T. Baker Inc., and 30% H_2O_2 from VWR. Glass microscope slides were obtained from Fisher Scientific. Nanopure water (> 18.0 MΩ) purified using the Millipore Milli-Q gradient system was used in all experiments.

Methods. As illustrated in Figure 1, the glass slide was cut to approximately 20 mm x 7 mm in size, to fit into the eppendorf test tube. After derivatization with APTMS, the glass surface was patterned by an adhesive tape cut with a V shape as shown in Figure 1. Following the Au colloid self-assembly and silver deposition steps, both clean glass and glass covered with Au-core Ag-shell nanoparticles were coated with FITC-HSA, by incubation of FITC-HSA at 4°C overnight, which forms a protein monolayer about 4 nm thick. This fluorescent monolayer makes it possible to quantitatively compare the fluorescence intensity of fluorophore-protein conjugates with and without silver nanostructures. The enhancement factor was determined as the ratio of fluorescence intensity on silver to fluorescence intensity on clean glass, given both surfaces are known to have almost equal monolayer coverage [9].

Characterization. Transmission electron microscopy was performed with a JEOL Model 1200 EXII system operating at 100 kV accelerating voltage. UV-visible extinction spectra were obtained using a Cary spectrophotometer (Cary 5000 UV-Vis-NIR Spectrophotometer). The glass substrates were maintained in an upright position in a solid sample holder. Scanning Electronic Microscopy images were collected using a

scanning electronic microscope (JEOL-JEM-1200 EX II model), equipped with an Energy Dispersive X-ray Analysis (EDX) system (Traktor TN-2000 energy dispersive spectrometer). Fluorescence images were captured by using Laser Scanning Microscopy SPM2 system (Leica Microsystems) with an electronically controlled acousto-optical beam splitter capable of a minimum bandwidth setting of 5 nm. The sample was excited with an Ar laser emitting at 488 nm and the emission was collected over a range of 600 nm to 660 nm.

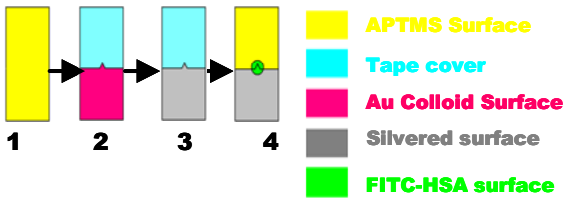

Figure 1. Schematic illustration of the deposition procedure for Au-core Ag-shell nanoparticles on glass surface (Top view). (1)APTMS modified glass surface; (2) Zero residual tape patterning and Au colloid depostion; (3) Silver enhancing deposition; (4) Patterning the interface with Press-to-seal silicone insulator; incubation with FITC-HSA.

III. Result and Discussions

The extinction spectrum of a typical Au colloid solution shows the extinction maximum at 519 nm and FWHM of 10 nm, which indicates the absence of aggregation of the synthesized Au colloid. The TEM images of these particles were recorded and their size distributions were obtained from at least 200 individual particles. This analysis shows that Au colloid had average diameter of 9 nm, with the standard deviation of 1.2 nm, implying that Au colloid solution was practically monodisperse. Using such monodisperse Au colloid as seed for silver deposition gives better prospects of size uniformity after the silver enhancement than with the conventional Ag colloid synthesis where strong size variations have been reported [10].

In the next step we employed the established technique of self assembly of Au colloid on glass surface, investigated earlier in SERS applications [11]. As shown in Figure 2A, the Au colloid was dispersed in a single layer on the glass surface. Individual particles in this layer were physically separated but small inter-particle distance ensured the strength of electromagnetic interaction. The particle attachment was made possible through the hydroxyl groups on the glass substrate surface which provided active sites for an alkoxysilane containing functional group, in this case, APTMS, which has a high affinity for Au. The self-assembled Au monolayers thus prepared were very stable owing to the following factors. First, the Au colloid tends to be tightly bound to the glass surface as numerous bonds are formed between Au nanoparticles and substrate surface estimated to be as high as 4.5 hydroxyl groups per nm^2 of the glass surface [12]. Secondly, thermodynamic stability of these surfaces is very high, thus the exchange with molecules in solution containing the same functional group practically does not occur [11]. Strong covalent bonds to the glass substrate reduce the surface mobility of the nanoparticles and thus prevent their spontaneous coalescence. Therefore, in the silver deposition step, the reduced silver only covers the Au colloid surface and does not change the location of bound colloidal Au. .

The silver deposition was done by applying the silver enhancer solution to Au colloids attached to the glass surface. The thickness of silver layer coating was controlled by the length of the silver enhancing step as this reaction could be simply interrupted by extensive rinse with water. Depending on the inter-particle distance of the Au colloid precursor, the maximum silver enhancing time was varied.

The process of silver enhancement can be understood as follows. A silver enhancer solution generally consists of silver ions and a reducing agent, buffered at an acidic pH. The reaction between silver ions and the reducing agent, silver nitrate and hydroquinone, respectively, for example, could be explained by the following equation[31]:

$$2AgNO_3 + C_6H_4(OH)_2 \rightarrow CO(CHCH)_2CO + 2HNO_3 + 2Ag\downarrow$$

The scanning electron micrographs (Figure 2B and 2C) show not only the size but also the surface morphology of the Au-core Ag-shell nanoparticle. They are approximately spherical, especially at short silver enhancing time. Upon close examination, the formed nanoparticles reveal a more complex shape, especially at longer silver enhancing times, which we will refer to as a nano-flower instead of a smooth spherical surface. The silver coating is believed to be homogeneous on Au core in initial stage; with increasing the enhancing time the silver nuclei then become new cores and thus the nano-flower shaped particles are formed. The average particle sizes, calculated from 100 particles, with 1 minute and 3 minutes silver enhancing time are about 19 nm and 47 nm respectively.

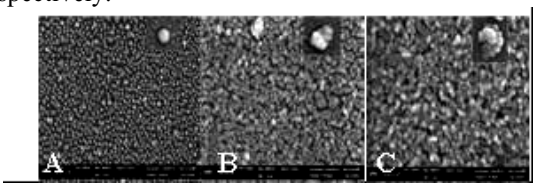

Figure 2. An SEM image of (A) 9 nm Au colloid; (B) Au-core Ag-shell nanoparticles after 1 minute silver enhancing step(~19 nm); (C) Au-core-Ag-shell nanoparticles 3 minutes silver enhancing step (~47 nm); inserts show the morphology of individual particles.

The composition of the nanostructure modified surface was tested by Energy Dispersive X-ray Analysis (EDX), and results are shown in Figure 3. In the range within 4 KeV, the characteristic peaks at 2.1 95KeV (M) and 2.984 KeV (K_α) of gold and silver, respectively, were observed. As shown in Figure 3A, in the 9 nm Au colloid, in addition to Si (K_α : 1.739 KeV) and C (K_α : 0.277 KeV) peaks, originating from the glass substrate and APTMS monolayer, a characteristic peak attributed to Au appears at 2.195 KeV. After the silver enhancing step, as shown in Figure 3B and 3C, the characteristic peak for silver at 2.984 KeV can be seen and its peak intensity increases with increasing silver enhancing time,

which suggests the silver content in nanoparticles has increased. This is consistent with the fact that the thickness of silver shell increases and the particle grows.

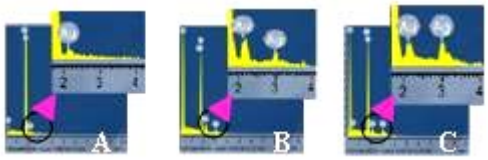

Figure 3. Energy Dispersive X-ray spectra of (A) 9 nm Au colloid; (B) Au-core-Ag-shell nanoparticles 1 minute silver enhancing (~19 nm); (C) Au-core-Ag-shell nanoparticles 3 minute silver enhancing (~47 nm); enlarged images show the increase in Ag content.

In addition to SEM and EDX characterizations, the UV-visible spectroscopy was used to record optical properties of the fabricated nanoparticles. The Au-core Ag-shell nanoparticles immobilized on glass surface showed characteristic surface plasmon peaks as shown in Figure 4. In contrast to the Au monolayer, which has a characteristic absorption peak at 519 nm, the Au-core silver-shell nanoparticles on glass substrate have two distinctive peaks at 394 nm and 595 nm for 19 nm nanoparticles, 394 nm and 635 nm for 47 nm nanoparticles, respectively. With increasing time of the silver enhancing step, and particle size, the absorption at these wavelengths is increased, with red shift of the long wavelength peak.

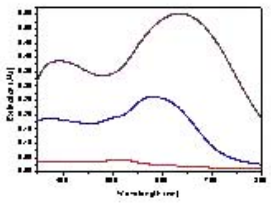

Figure 4. The UV-Visible spectra for the Au colloid dominated by absorption (red); silvered Au colloid with 1 minute silver enhancing time showing strong absorption and scattering (blue); and silvered Au colloid after 3 minutes silver enhancing time – dominated by scattering (purple).

The fluorescence images corresponding to each of the UV-visible spectra, (Figure 5) have also been recorded for each sample. As mentioned in experimental section, the laser scanning microscopy measurements were carried out after the samples were incubated with FITC-HSA to form a complete monolayer in the confined area, which included both metalised and clean glass surface. Figure 5A shows that the fluorescence intensity from FITC in the triangular area covered with the Au colloid monolayer is lower than that of the surrounding glass surface used as control. As shown in Figure 5B for the Au-core Ag-shell nanoparticles produced with 1 minute silver enhancing step the fluorescence signal from silvered surface is comparable with that from glass surface. When the silver enhancing time was increased to 3 minutes and hence the size of the nanoparticles increased to 47 nm, the fluorescence signal observed from the silvered area is much higher than that from glass surface, thus demonstrating fluorescence enhancement. This result unambiguously suggests that, depending on size of nanoparticles, the fluorescence of FITC was either quenched, very little affected or, enhanced in comparison to the control area, where fluorescence was due to FITC-HSA monolayer on bare glass surface. Such effect of nanoparticles on fluorescence is attributed to the interplay of two principal factors: the change of excitation rate caused by local electromagnetic field enhanced by interaction of an incident light with the metal nanoparticles and the (detrimental) change of quantum yield due to the effect of metals on the intrinsic decay rate of the fluorophore [13].

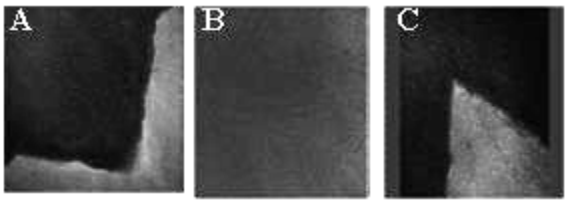

Figure 5. Laser scanning microscopy image of FITC-HSA monolayer on both nanoparticles and glass surface; excitation: 488nm, emission collection 520-560 nm; (A) 9 nm Au colloid as MEF substrate, shows fluorescence quenching; (B) Au-core-Ag-shell nanoparticles 1 minute silver enhancing step (nanoparticles size: 19nm) as a MEF substrate, almost no change of fluorescence; (C) Au-core-Ag-shell nanoparticles after 3 minutes Silver enhancing step (nanoparticles size: 47 nm) as a MEF substrate, clear fluorescence enhancement.

The fluorescence enhancement is known to correlate with the extinction properties of metal particles which are due to two contributions, from absorption (C_A) and scattering (C_S) [14-18]. The scattering component of the extinction relates to extent by which the plasmons can radiate the energy as a far-field propagating wave. When a metal particle is spherical and has a size comparable to the incident wavelength, its optical properties agree reasonably well with Mie theory. We note that our nanoparticles are less than 100 nm in size, where Mie theory reaches its limits, but despite that it has been widely used to describe properties of such colloids [8]. Based on this theory, the extinction cross section for a particle with a dielectric constant ε_1, is given by:

$$C_E = C_A + C_S = k_1 \, \mathrm{Im}(\alpha) + k_1^4 \, |\alpha|^2 / 6\pi \qquad (1)$$

where $k_1 = 2\pi \, n_1/\lambda_0$ is the wavevector of the incident light in medium 1 and α is the polarizability of the sphere of radius r,

$$\alpha = 4\pi r^3 \, (\varepsilon_m - \varepsilon_1)/ (\varepsilon_m + 2\varepsilon_1) \qquad (2)$$

where ε_m is the complex dielectric constant of the metal. In Eq. 1, the first term corresponds to the cross section due to absorption and the second term represents the cross section due to scattering. It was suggested the absorption term C_A is linked to quenching while the scattering term C_S is linked to enhancement in surface enhanced fluorescence [13]. Eqs. 1 and 2, show that C_A increased as r^3 whereas C_S increases as r^6,. This implies that small metal particles are expected to quench fluorescence because absorption dominates over the scattering, while larger metal particles are expected to enhance fluorescence because the scattering component is dominant over the absorption.

On the basis of these considerations, the effect of silvered Au colloid on fluorescence can be correlated with the UV-visible spectra shown in Figure 4 where the scattering component and the absorption component of the extinction

spectra can be separately analysed. For the Au colloid, the absence of the scattering component and the domination by the absorption with maximum at 519 nm [11], is consistent with its quenching effect on fluorescence. Based on theoretical calculation, the scattering efficiency for 9 nm Au colloid is almost 0 [17]. After 1 minute silver enhancing step, the extinction spectrum shows that, in addition to absorption peak centered at 394 nm, which partially contributes to the absorption component, a new peak at 595 nm appeared which could be attributed to scattering.. The scattering efficiency for 19 nm Ag colloid is about 2.1 [17]. However, it is difficult to predict whether this colloid will act as a quencher or enhancer of fluorescence due to the existence of both absorption and scattering components. With increasing size of silvered Au colloid, the scattering component becomes dominant over the absorption component; and scattering efficiency is increased, with the value of 6 given in Ref [17] for the nanoparticle size of 40 nm. This correlates with enhancement of fluorescence on such nanoparticles, which was confirmed by the fluorescence image shown in Figure 7C. These results are in good agreement with earlier reports [8].

The enhancement factor was determined as the ratio of fluorescence intensity on silvered surface to the fluorescence intensity on glass surface, given both surfaces are known to have complete monolayer coverage [19]. As shown in Figure 6, the enhancement factor for the silvered sample with 3 minutes silver enhancing time is over 11. This observed increase of fluorescence intensity can, in principle be attributed to geometrical effects such as an increased surface area, and we note most of other reports state the same fluorophore coverage on both silvered and glass surface [20-23]. We have accounted for such geometrical factors by calculating the total radiant flux emitted by the fluorophore layer covering our nanostructures. This is a more exact approach compared with the calculation of the surface area. of the flat surface occupied by that sphere (equal to its cross-section).

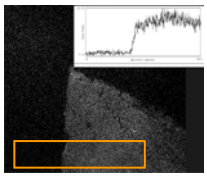

Figure 6. Fluorescence enhancement profile of Figure 5c.

The final comparison was made between the flux from the modeled nano-flower compared with the flux from the flat square surface area which is required to accommodate this nano-flower, where the factor of 1.9 was obtained. This means that the presence of nano-flowers on the surface can only account for about 90% increase in fluorescence intensity, with the remaining factor of about 6 attributable to fluorescence enhancement.

IV. Conclusions

A fast and simple method has been proposed for producing homogeneous silvered nanostructures on glass surface as a substrate for fluorescence enhancement. Depending on size of these nanoparticles, the fluorescence of FITC was either quenched, not affected or, enhanced in comparison to the control area. The Au-core-Ag-shell nanostructures with 3 minutes silver enhancing time had the enhancement factor of over 10, which can produce technologically promising substrates for fluorescence enhancement. It was shown that the enhancement factor is much higher than the predictions based on the increase of surface area alone. One of the key advantages of substrate prepared in this way was macroscopic uniformity of the surface.

Acknowledgment

The first author would like to acknowledge the support from International Macquarie University Research Scholarship and Macquarie University Biotechnology Research Institute (MUBRI).

References

[1] Kronick M.N. J. Immunol. Methods, 92, 1, 1986

[2] Gosling J.P.A. Cell, 36, 1408, 1990

[3] Lövgen T; Pettersson K. Fluorescence Immunoassay and Molecular Applications, Van Dyke K, Van Dyke R. Eds, CRC Press, New York, p234-250, 1990

[4] Casay G.A.; Shealy D.B.; Patonay G. Vol. 4, Probe Design and Chemical Sensing, Lakowicz JR Ed., Plenum Press, New York, 1994

[5] Daehne S.; Resch-Genger U.; Wolfbeis O.S. Eds. Near-Infrared Dyes for High Technology Applications, Kluwer Academic Publishers, New York, 1998

[6] Walker N.J., Science, 296, 557, 2002

[7] Aslan K, Lakowicz JR, Geddes CD, Anal. Bioanal. Chem. 382, 926-933, 2005

[8] Lakowicz J.R., Anal. Biochem 337, 171-194, 2005

[9] Lakowicz J.R.; Malicka J.; D'Auria S.; and Gryczynski I. Anal. Biochem., 320, 13, 2003

[10] Huang T.; Murray R.W. J Phys Chem B,105, 12498, 2001

[11] Grabar K.C.; Freeman R.G.; Hommer M.B.; and Natan M.J. Anal. Chem., 67, 735-743, 1995

[12] Kruger A.A.; Surface and Near-Surface Chemistry of Oxide Materials, Nowotny J, Dufour LC Eds, Elsevier Science Publishers, Amsterdam, pp 413-448, 1988

[13] Lakowicz, J.R.; Geddes C.D.; Gryczynski I.; Malicka J.; Gryczynski Z.; Aslan K.; Lukomska J.; Matveeva E.; Zhang J.; Badugu R.; and Huang J. J. Fluoresc., 14, 425, 2004

[14] Kreirib U.; Vollmer M.; Optical Properties of Metal Clusters, Springer, Berlin, p. 532, 1995

[15] Feldheim D..L.; Foss C.A. Metal Nanoparticles: Synthesis, Characterization and Applications, Marcel Dekker Inc., New York, p. 338, 2002.

[16] Kerker M.; Blatchford C.G., Phy. Rev. B, 26, 8, 4052, 1982

[17] Ygurabide J.; Ygurabide E., Anal. Biochem., 262, 137, 1998

[18] Ygurabide J.; Ygurabide E., Anal. Biochem., 262, 157, 1998

[19] Malicka J.; Gryczynski I.; Geddes C.D.; Lakowicz J.R. J. Biomed. Opt., 8(3), 472, 2003

[20] Sokolov K.; Chumanov G.; Cotton T..M., Anal. Chem., 70, 3898, 1998

[21] Geddes C.D.; Cao H.; Gryczynski I.; Gryczynski Z.; Fang J.; Lakowicz J.R., J Phys Chem A, 107, 3443, 2003

[22] Aslan K..; Leonenko Z.; Lakowicz J.R.; Geddes C.D. J Phys Chem B, 109, 3157, 2005

[23] Aslan K.; Lakowicz J.R.; Geddes C.D.;, J Phys Chem B, 109, 6247, 2005